

Preparation of anticorrosive cobalt-doped ZnO nano pigments by a combustion method; A comparison study between microwave irradiation and a conventional heating source

Sousan Rasouli*

Department of Nanomaterials & Nanocoatings, Institute for Color Science and Technology, 55 Vafamanesh Ave., HosseinAbad Square, Pasdaran St, 1668814811, Tehran, Iran

In the present study, cobalt-doped ZnO nano pigments were synthesized by a solution gel combustion method using glycine fuel. A chamber furnace and microwave irradiation were used as heating sources. Products were characterized by X-ray diffraction, scanning-transmission electron microscopy and diffuse reflectance. The anticorrosive properties of the pigments obtained were investigated by electrochemical impedance spectroscopy. The results have shown that using glycine as the fuel pure ZnO phase was obtained directly by the two heating sources. Electron microscopy demonstrated quasi-spherical particles with a crystallite size of 49 nm for furnace-assisted and rod-like particles of 63 nm for the microwave-assisted procedure were obtained. The corrosion performance of the coating in 3% w/V NaCl solution was evaluated by electrochemical impedance spectroscopy (EIS) and polarization measurements. According to the measurements of EIS and electrochemical polarization, the coatings with a furnace-assisted pigment showed a higher corrosion resistance.

Key words: Solution combustion, Furnace, Microwave, Anticorrosive, Mild steel electrode.

Introduction

Numerous synthesis techniques such as sol-gel [1], precipitation [2], solid-state reaction [3] and combustion synthesis [4-5] have been used to prepare fine ceramic pigments. Among them, the solution combustion method is one of the most interesting synthesis routes for production of homogenous nano-crystalline single and multi-component oxides. The ability to achieve high purity single and multiphase complex oxide powders is the great advantage of this technique for the preparation of ceramic materials. This process is based on an exothermic reaction of metallic nitrates with a fuel at low temperatures. After adding metallic nitrates and fuel to deionized water and evaporation of the excess water a highly viscous precursor gel is gained. Then, a heating source is necessary to complete the combustion reaction. The initial combustion process used a conventional furnace as a heating system. However, this heating method has some inconveniences such as being time consuming and giving a non-homogeneous product.

Recently a novel technique called 'microwave-assisted combustion synthesis' has been used to synthesize oxide materials [6]. Microwave heating can be more advantageous than conventional heating because of a short processing time and volumetric heating [7]. Microwaves are electro-

magnetic waves that have a frequency range of 0.3 to 300 GHz and corresponding wavelengths ranging from 1 m to 1 mm. A Typical frequency for a material process is 2.45 GHz. It has long been established that dielectric materials, such as many types of ceramics can be heated with energy in the form of microwaves [8]. Zavyalova *et al.* investigated the microwave-assisted self-propagating combustion synthesis for the uniform deposition of metal nanoparticles on ceramic monoliths [9]. Sutton was the first researcher who reported the phenomenon that ceramic materials were heated by microwave energy [10]. There are several reasons for the growing interest in microwave processing over the conventional processing method, including the potential for significant reductions in the manufacturing costs due to energy savings and a shorter processing time. This process improves product uniformity and yield, provides unique microstructures and properties due to selective heating.

In this paper, the use of high power microwave energy for the synthesis of cobalt-doped ZnO nano pigments is described and the results are compared to ones by a conventional furnace heating source. X-ray diffraction, scanning-transmission electron microscopy, diffuse reflectance and electrochemical impedance spectroscopy (EIS) were used to characterize the properties of products.

Experimental

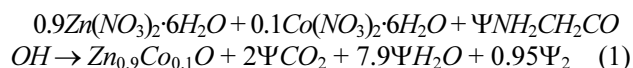
Materials and methods

All the materials used in this study were of analytical grade. Previous work had demonstrated that for a solid

*Corresponding author:
Tel : +98-21-229-52272
Fax: +98-21-229-47537
E-mail: rasouli@icrc.ac.ir

state reaction a complete solid solution of ZnO-Co can be achieved by the addition of 0-20% of Co_3O_4 [11]. Since low amounts of cobalt (less than 5%) are not detectable by XRD, 10 wt% Co was used to insure pure formation of a solid solution. In this case, $\text{Zn}_{0.9}\text{Co}_{0.1}\text{O}$ was considered as the stoichiometric composition.

The exothermic redox stoichiometric reactions between oxidizer (zinc nitrate) and fuel (glycine) to achieve $\text{Zn}_{0.9}\text{Co}_{0.1}\text{O}$ composition can be expressed as follows [12]:



where the Ψ represents the ratio at which the value of the oxygen balance is equal to zero.

Stoichiometric amounts of $\text{Zn}(\text{NO}_3)_2 \cdot 6\text{H}_2\text{O}$ and $\text{Co}(\text{NO}_3)_2 \cdot 6\text{H}_2\text{O}$ were completely dissolved in deionized water in a beaker. Then, glycine fuel was slowly introduced to the solution under vigorous stirring and the temperature increased up to 90 °C. After 30 minutes, the solution completely converted to a highly viscous gel. The beaker was transferred to a heating source being; a chamber furnace and a microwave oven to complete the combustion reaction. The combustion reaction time was 30 minutes and 50 seconds for the chamber furnace and microwave oven, respectively. The synthesized samples were coded as; CF and MO for chamber furnace and microwave oven samples, respectively.

Corrosion tests

As-prepared pigments were incorporated in an alkyd-based coating system at 2 wt%. The dispersion was done using a mechanical stirrer followed by ultrasonication. The nano-composite coating was applied on pretreated steel test panels (76.2 mm × 152.4 mm × 0.8 mm) by an appropriate applicator.

A steel sheet was used as the working electrode. The exposed surface area of each electrode was 1 cm. Prior to coating the surface, the surface pretreatment of the working electrode was performed by mechanical polishing of the electrode surface with successive grades of emery papers down to 1200 grit up to a mirror finish. The electrode was then, rinsed with acetone and distilled water before film formation. The experiments were performed in a 100 cm volume cell at 20 °C, using platinum and calomel as auxiliary and reference electrodes, respectively. The experiments were carried out in a 3% w/V NaCl solution. All solutions were freshly prepared from analytical grade chemical reagents (Merck) using doubly-distilled water and were used without further purification. For each run, a freshly prepared solution as well as a new sample electrode was used.

Characterization techniques

The powders obtained were characterized by X-ray diffraction using A D-500 (Siemens, Karlsruhe, Germany) diffractometer. The morphology and size of different

samples were performed by a LEO 1455 VP scanning electron microscope (SEM) and a transmission electron microscopy (TEM) (Zeiss, Em 900). The color properties of the products obtained were determined by ultraviolet radiation spectroscopy in the visible-ultraviolet light region. Diffuse reflectance was determined with a Color Eye 7000 A spectrometer in the range between 300 and 700 nm.

Electrochemical studies were carried out in a conventional three electrode cell powered by an electrochemical system comprising of an EG&G model 273 potentiostat/galvanostat and a solartron model 1255 frequency response analyzer. The system was run by a PC through M270 and M398 commercial software via a GPIB interface.

Results and Discussion

Pigments characteristics

Fig. 1 shows the XRD patterns of the synthesized powders obtained using a chamber furnace (CF) and a microwave oven (MO) as heating sources. It is observed that a very intense single hexagonal ZnO phase with a P63mc structure (JCPDS 5-664) was obtained for both samples. Moreover, the extremely broad peaks about 32 and 36° indicate the nano-crystalline nature of the ZnO phase. The average crystallite size (D) was determined by Debye-Scherrer's formula according to equation 2:

$$D = \frac{0.9\lambda}{\beta \cos\theta} \quad (2)$$

where λ is the wavelength of incident X-rays, β is the half width of the diffracted peak and θ is the diffracted angle.

The average crystallite size was calculated as 49 and 63 nm for the CF and MO samples, respectively. In fact, decomposition of glycine occurred at a lower temperature and the energy released from the redox reaction of the glycine fuel and zinc and cobalt nitrates accelerated the phase formation of ZnO. However, crystal growth is more favorable in the case of the microwave heating system. This can be related to the large amount of energy

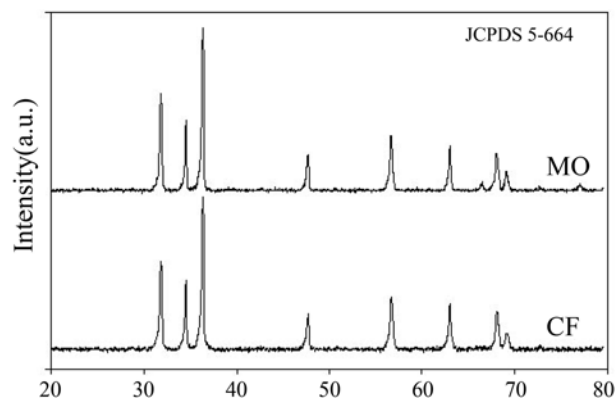
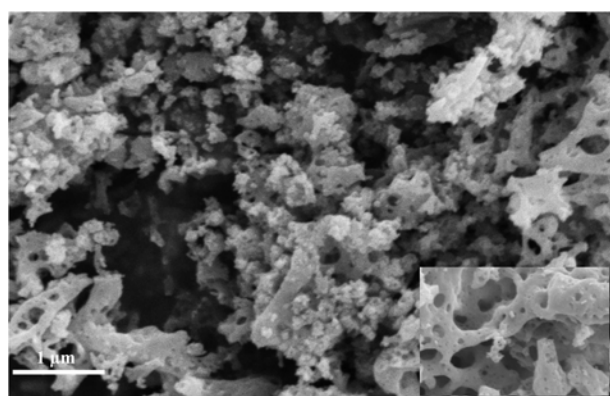


Fig. 1. XRD pattern of Zn O-Co prepared by FC) furnace assisted, MO) microwave assisted combustion methods.

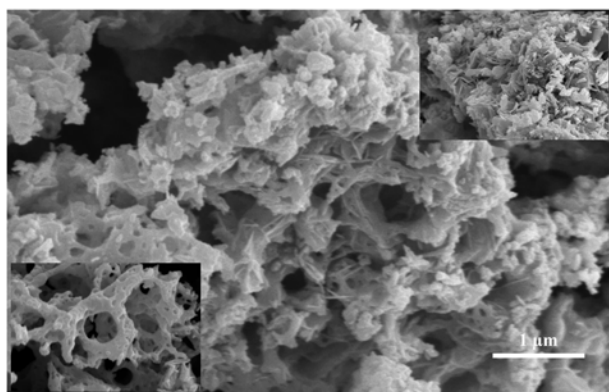
(from the redox reaction of the glycine fuel and zinc and cobalt nitrates) released in a short time leading to crystal growth.

Fig. 2(a)-(b) show typical SEM images of the as-synthesized ZnO-Co powders with; chamber furnace (2a) and microwave oven (2b) heating sources. Fig. 2(a) shows that the as-prepared ZnO-Co with a chamber furnace is entirely spongy and porous with a pore size about 0.1-0.5 μm . The spherical polycrystalline aggregates or semi-spherical particles appearing in Fig. 2(a) sample is due to radiating growth from the center [13]. The as-prepared ZnO-Co with a microwave oven has more complicated appearance and a mixture of localized semi-sintered particles and flake-like morphologies is observed in the sample. In fact, the energy released from the combustion reaction is associated with an enhancement of amine groups as a result of the glycine fuel [14]. When the ignition of metal nitrates starts in the presence of nitrogen-based fuels, localization of heat on the particle boundaries results in the semi-sintered particles observed in Fig. 2(a). The longer time of the reaction in the case of the furnace heating source can be favorable to the efficiency of such localized heating zones leading to the formation of more semi-spherical particles.

TEM images of ZnO-Co powders synthesized by the different heating sources are shown in Fig. 3(a)-(b). As

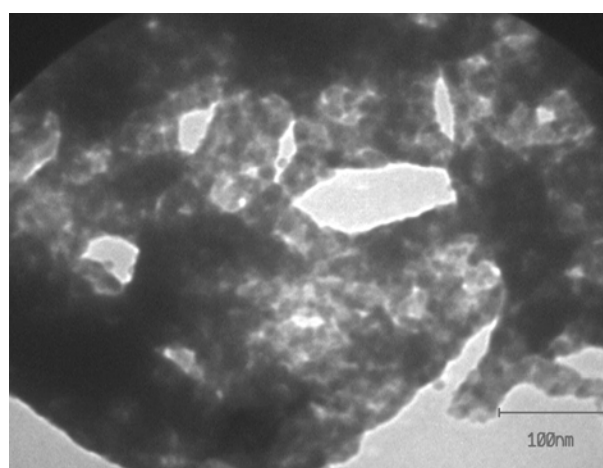


(a)

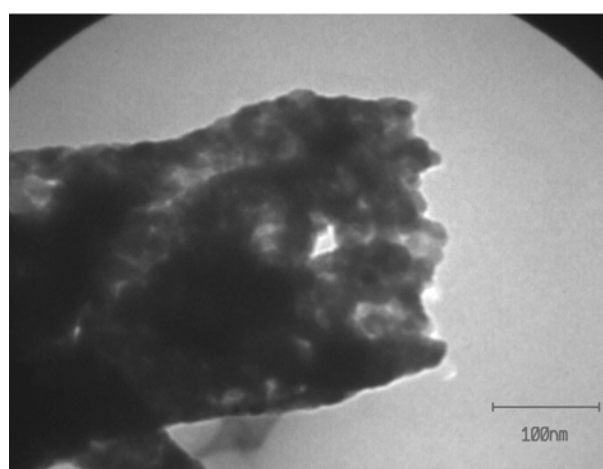


(b)

Fig. 2. SEM images of the as-synthesized samples, (a) furnace assisted, (b) microwave assisted combustion method.



(a)



(b)

Fig. 3. TEM images of the samples (a) furnace assisted, (b) microwave assisted combustion method.

shown in figures large amounts of exhaust gases led to the formation of loose packed agglomerates whose size is less than 50 nm.

The color properties of the synthesized samples have been investigated by ultraviolet radiation spectroscopy in the visible-ultraviolet light region. Diffuse reflectance curves are plotted in Fig. 4. According to the figure, a broad reflection band around 530 nm, a characteristic peak for the green region, can be observed for both samples. Cunha *et al.* [15] showed that the saturated green color of a cobalt-doped ZnO pigment was obtained only with a complete entrance of cobalt into the ZnO structure. They have reported this observation by investigating the effect of the calcination temperature on the color of the samples due to the complete or partial entrance of cobalt into the ZnO structure.

Anticorrosion investigation

In order to study the influence of the inhibitors on the corrosion resistance of steel panels, a potentiodynamic study has been performed on steel in NaCl solutions for

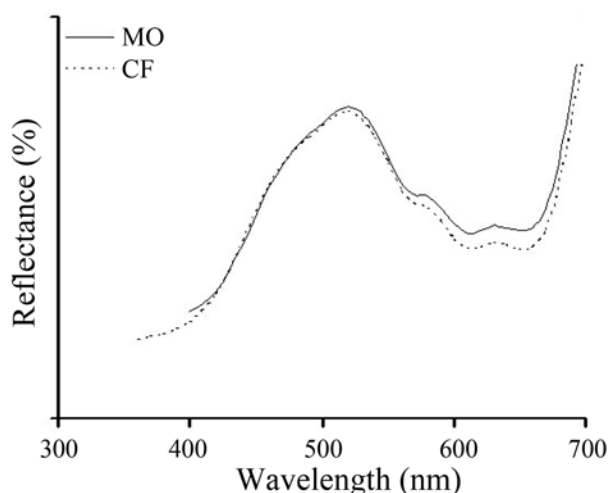


Fig. 4. Diffuse reflectance curves for CF and MO samples.

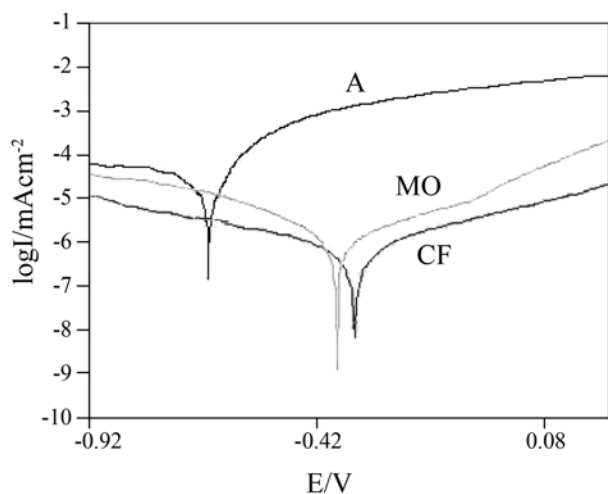


Fig. 5. Typical potentiodynamic anodic and cathodic polarization curves recorded for steel in 3% w/V NaCl solution in the absence and presence of the inhibitor on the surface of an electrode.

pigments prepared by furnace and microwave heating sources and the results were compared to bare electrodes without any pigment. Fig. 5 shows typical potentiodynamic polarization curves recorded for a steel electrode in a solution containing 3% w/V NaCl for different prepared samples with and without pigments: CF; the pigment from the chamber furnace, MO; the pigment from the microwave oven and A; film without any pigment. The polarization curves show Tafel type behavior of these samples. Tafel calculations are listed in Table 1, where E_{corr} , I_{corr} , β_a , β_c

and IE ($IE = (I_{blank} - I_{inhi}) / I_{blank}$) [16] are the corrosion potential, corrosion current density, corrosion rate, anode Tafel constant, cathode Tafel constant and inhibition efficiency, respectively.

The open circuit corrosion potentials, E_{corr} , are drifted to more positive values and a significant decrease of the corrosion current was observed on the steel substrate in the presence of MO and CF pigments. These results indicate that these inhibitors act generally as an anodic inhibitor. According to the data of Table 1, it is obvious that in the presence of the inhibitor, the corrosion rate of the samples decreases in the order of $A > MO > CF$. Therefore, the CF has the most corrosion resistance in the NaCl solution.

Fig. 6 shows typical potentiodynamic polarization curves recorded for steel electrodes in a solution containing 3% w/V NaCl in the absence and presence of CF and MO after seven days immersion. As can be seen, after seven days the protective effect of the inhibitor layer of CF and MO was not obviously changed. Tafel calculations after seven days immersion are listed in Table 2. It seems that semi-spherical particles have a better corrosion inhibition surface than the flake-like ones. This can be due to the better adhesion and compression of these particles with a mean particle size of 50 nm. On the other hand, this phenomenon can be explained easily by filling free spaces between particles of smaller sizes. With flake-like particles, the filling of pores by means of the oxide is incomplete

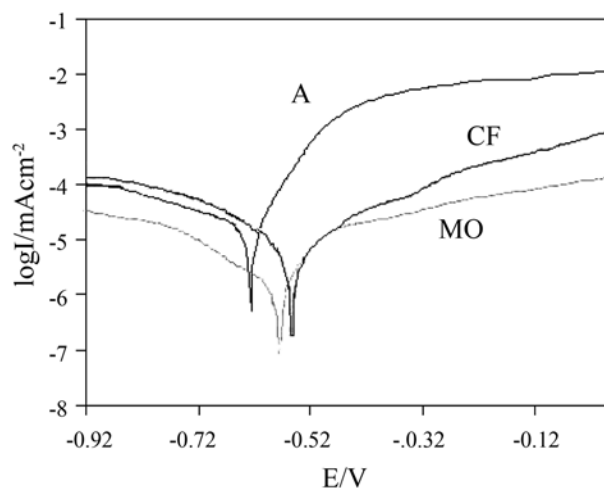


Fig. 6. Typical potentiodynamic anodic and cathodic polarization curves recorded for steel after 7 days immersion of electrodes in a 3% w/V NaCl solution in the absence and presence of the inhibitor on the surface of an electrode.

Table 1. Polarization parameters in the corrosion of steel electrodes in a 3% wV NaCl solution in the absence and presence of inhibitors at 25 °C

sample	E_{corr}/mV	$I_{corr}/mAcm^{-2}$	Tafel slope $\beta_a/mVdec^{-1}$	Tafel slope $\beta_c/mVdec^{-1}$	IE%
A	-657	15.8	181	640	-
MO	-375	0.5	287	275	0.95
CF	-315	0.27	151	149	0.97

Table 2. Polarization parameters in the corrosion of steel electrodes after 7 days immersion in a 3% w/V NaCl solution in the absence and presence of inhibitors at 25 °C

sample	$E_{\text{corr}}/\text{mV}$	$I_{\text{corr}}/\text{mAcm}^{-2}$	Tafel slope $\beta_a/\text{mVdec-1}$	Tafel slope $\beta_c/\text{mVdec-1}$	IE%
A	-625	19.9	101	629	-
MO	-575	1.25	125	205	0.93
CF	-538	0.68	107	173	0.95

and the leakages can lead to more easy liquid and gas penetrations through the paint film. With particles of flake-like or rode-like type the sealing of rather voluminous pores in the coating is difficult, and the coatings exhibit a lower anticorrosion efficiency.

Conclusions

ZnO-Co green ceramic pigments were successfully synthesized by a solution gel combustion method using a conventional furnace and microwave irradiation heating sources. X-ray results have shown with glycine as fuel a pure ZnO phase was obtained directly for the two heating sources. The results demonstrated that the heating method can influence the crystallite size and particles shape.

Investigations of the corrosion inhibition of steel electrodes in a solution containing chloride ions through electrochemical methods demonstrated that the coatings with a furnace-assisted pigment showed better corrosion resistance and a lower corrosion current. It was revealed that these coatings were more compact and uniform than the coatings with a microwave-assisted pigment.

References

1. R. Ricceri, S. Ardizzone, G. Baldi and P. Matteazzi, *J. Eur. Ceram. Soc.*, 2 (2002) 629-637.
2. I.S. Ahmed, H.A. Dessouki and A.A. Ali, *Spec. Acta Part A, Mol. and Biomol. Spec.*, 71[2] (2008) 616-620.
3. S.T. Aruna, S. Ghosh and K.C. Patil, *Inter. J. Inorg. Mat.*, 3[6] (2001) 387-392.
4. S.T. Aruna and A.S. Mukasyan, *Current Opinion in Solid State and Materials Science*, 12 (2008) 44-50.
5. C.C. Hwang, T.Y. Wu, J. Wan and J.S. Tsai, *Materials Science and Engineering B* 111 (2004) 49-56.
6. D.Y. Chung and E.H. Lee, *Journal of Alloys and Compounds*, 374 (2004) 69-73.
7. A. Lagashetty, V. Havanoor, S. Basavaraja, S.D. Balaji, A. Venkataraman, *Science and Technology of Advanced Materials*, 8[6] (2007) 484-493.
8. D.E. Clark, I. Ahmad and R.C. Dalton, *Materials Science and Engineering: A*, 144 (1991) 91-97.
9. U. Zavyalova, F. Girgsdies, O. Korup, R. Horn and R. Schlgl, *J. Phys. Chem. C*, 113[40] (2009) 17493-17501.
10. W.H. Sutton, *Am. Ceram. Soc. Bull.*, 68 (1989) 376-386.
11. A. Varma and A.S. Mukasyan : *Korean Journal of Chemical Engineering*. 21[2] (2004) 527-536.
12. C.S. Lin, C.C. Hwang, W.H. Lee and W.Y. Tong : *Materials Science and Engineering B*. 140 (2007) 31-37.
13. S.K. Sharma, S.S. Pitale, M.M. Malik, R.N. Dubey, M.S. Qureshi and S. Ojha, *Physica .B*. 405 (2010) 866-874.
14. F. Li, K. Hu, J. Li, D. Zhang and G. Chen, *J. Nucl. Mater.* 300 (2002) 82-88.
15. J.D. Cunha, D.M.A. Melo, A.E. Martinelli, M.A.F. Melo, I. Maia and S.D. Cunha: *Dyes and Pigments*. 65 (2005), 11-14.
16. J.Z. Ai, X.P. Guo and Z.Y. Chen, *J. Appl. Surf. Sci.*, 253 (2006) 683-688.